PHYSICAL REVIEW D **91,** 054018 (2015)

Wigner distributions for gluons in a light-front dressed quark model

Asmita Mukherjee, Sreeraj Nair, and Vikash Kumar Ojha
Department of Physics, Indian Institute of Technology Bombay, Powai, Mumbai 400076, India
(Received 27 January 2015; published 13 March 2015)

We present a calculation of Wigner distributions for gluons in a light-front dressed quark model. We calculate the kinetic and canonical gluon orbital angular momentum and spin-orbit correlation of the gluons in this model.

DOI: 10.1103/PhysRevD.91.054018 PACS numbers: 12.38.-t, 12.38.Bx, 13.88.+e

I. INTRODUCTION

To have a complete understanding of matter at the subatomic level, it is important to understand the nucleon spin structure. This means understanding how the spin ($\frac{1}{2}$) of the nucleon is shared by the quarks and gluons in the nucleon and what contribution is made by their orbital angular momentum (OAM). Earlier it was believed that all nucleon spin is carried by quarks. The EMC experiment showed that the contribution of quark spin to nucleon spin is very small. So, an important question is, where does the missing (remaining) angular momentum come from? As the nucleon is made up of quarks and gluons, it is natural to expect that the missing angular momentum comes either from gluon spin or from quark or gluon OAM. This is expressed by the spin sum rule [1]:

$$\frac{1}{2}=\frac{1}{2}\sum_q \Delta q+\underbrace{\sum_q \mathcal{L}^q}_{\text{quark OAM}}+\Delta G+\underbrace{\mathcal{L}^g}_{\text{Gluon OAM}}.$$

Here $\frac{1}{2}\sum_q \Delta q$ and ΔG are the quark and gluon spin angular momentum, respectively. The above sum rule is called the canonical spin sum rule. Except for the quark intrinsic part, the terms depend upon specific gauge choice.

Recently, Chen *et al.* [2] introduced a gauge-invariant extension (GIE) which is basically a prescription to find a manifestly gauge-invariant quantity that coincides with a gauge-noninvariant quantity in a particular gauge. In this way, one can extend to any other gauge the validity of a physical interpretation of the canonical OAM $\mathcal{L}^q$ and $\mathcal{L}^g$ in the light-front gauge. There is another decomposition called the kinetic decomposition of nucleon spin [3],

$$\frac{1}{2}=S^q+L^q+J^g,$$

where S^q and L^q are quark spin and kinetic orbital angular momentum, respectively. J^g is the total gluon contribution to the angular momentum of the nucleon. Later, Wakamatsu [4] further separated the J^g into a gluon orbital part (L^g) and an intrinsic part (S^g), using a prescription similar to [2]. Which of the two definitions of the OAM is "physical" is a matter of intense debate. According to the current understanding, the difference between kinetic and canonical OAM is the choice of the Wilson line in the definition of the nonlocal quark operator: a staple-type gauge link gives the canonical OAM, whereas a straight line gauge link gives the kinetic OAM. An interesting physical interpretation of both types of OAM is given in [5,6].

Recently it has been shown that the Wigner distribution can provide useful information on the spin and angular momentum correlation of quarks and gluons in the nucleon. Wigner distributions [7] are quasiprobabilistic distributions in which both position and momentum space information are encoded. They are directly related to generalized parton correlation functions (GPCFs) [8]. GPCFs are fully unintegrated, off-diagonal, quark-quark correlators and contain the maximum amount of information about the structure of the nucleon. If we integrate GPCFs over the light cone energy (k^-), we get generalized transverse momentum-dependent parton distribution functions (GTMDs). These GTMDs are Fourier transforms of Wigner distributions and vice versa.

In fact, the GTMDs are directly related to generalized parton distributions (GPDs) [3] and transverse momentum-dependent parton distribution functions (TMDs) [8], both of which have been found to give very useful information about the structure and spin of the nucleon in terms of quarks and gluons. We can take two-dimensional Fourier transforms of GPDs with respect to the momentum transfer in the transverse direction to get impact parameter-dependent parton distribution functions (IPDPDFs) [9]. These give the correlation in transverse position and longitudinal momentum for different quark and target polarizations. On the other hand, TMDs provide momentum space information and also the strength of spin-orbit and spin-spin correlation. It has been shown that both of these distributions are linked to GTMDs. So we can consider the GTMDs or, equivalently, Wigner distributions as mother distributions.

Wigner distributions, described above, are joint position and momentum space distributions of quarks and gluons in the nucleon. Due to the uncertainty principle, they are not positive definite and do not have probabilistic interpretations. However, integration of Wigner distributions over one or more variables relates them to measurable quantities [10]. Here, model calculations of Wigner functions are

important as these calculations play a significant role in revealing what kind of information they can provide about the correlations of quarks and gluons inside the nucleon. Also, such calculations are useful for checking various relations among the GTMDs and the TMDs and GPDs. In fact, some relations have been found to hold only in a certain class of models [11]. In this work, we calculate the Wigner distributions in the light-front Hamiltonian approach [12]. This approach gives an intuitive picture of deep inelastic scattering processes, as it is based on field theory but keeps close contact with parton ideas [13]. Here the partons, i.e., quarks and gluons, are noncollinear, massive, and they also interact. The target state is expanded in Fock space in terms of multiparton light-front wave functions (LFWFs). The advantage of using light-front (infinite momentum frame) formalism is that such wave functions are boost invariant, so one can work with a finite number of constituents of the nucleon, and this picture is invariant under Lorentz boost [14]. In order to obtain the LFWFs of the nucleon, one needs a model light-front Hamiltonian. However, much useful information can be obtained if one replaces the bound state by a simple spin-$\frac{1}{2}$ composite relativistic state like a quark at one loop dressed with a gluon [15,16]. In our previous work [17], we studied the Wigner distribution of quarks for a simple relativistic spin-$\frac{1}{2}$ composite system, namely, for a quark dressed with a gluon, using the light-front Hamiltonian perturbation theory. Here we calculate the Wigner distribution for gluons in the same model. This calculation is useful because in most commonly studied phenomenological models, gluonic degrees of freedom are not present [10], and a study of the gluon spin and OAM is not possible there.

II. WIGNER DISTRIBUTIONS

The Wigner distribution for gluons can be defined as [18]

$$xW^g(x,\vec{k}_\perp,\vec{b}_\perp)=\int\frac{d^2\vec{\Delta}_\perp}{(2\pi)^2}e^{-i\vec{\Delta}_\perp.\vec{b}_\perp}\int\frac{dz^-d^2z_\perp}{2(2\pi)^3p^+}e^{ik.z}\left\langle p^+,\frac{\vec{\Delta}_\perp}{2},\sigma\left|\Gamma^{ij}F^{+i}\left(-\frac{z}{2}\right)F^{+j}\left(\frac{z}{2}\right)\right|p^+,-\frac{\vec{\Delta}_\perp}{2},\sigma\right\rangle\Bigg|_{z^+=0}, \quad (1)$$

where $\vec{\Delta}_\perp$ is the transverse momentum transfer from the target state, and $\vec{b}_\perp$ is a two-dimensional vector in impact parameter space conjugate to $\vec{\Delta}_\perp$. We calculate Eq. (1) for $\Gamma^{ij}=\delta^{ij}$ and $\Gamma^{ij}=-i\epsilon^{ij}_\perp$.

We have

$$F^{+i}=\partial^+A^i-\partial^iA^+ + gf^{abc}A^+A^i.$$

The gauge field can be written as [13], for $i=1,2$,

$$A^i\left(\frac{z}{2}\right)=\sum_\lambda\int\frac{dk^+d^2k_\perp}{2k^+(2\pi)^3}[\epsilon^i_\lambda(k)a_\lambda(k)e^{-\frac{i}{2}k.z}+\epsilon^{*i}_\lambda(k)a^\dagger_\lambda(k)e^{\frac{i}{2}k.z}].$$

We choose the light-front gauge, $A^+=0$, and take the gauge link to be unity.

In our previous work [17], we calculated the quark Wigner distributions for a quark state dressed with a gluon. In this work, we investigate the gluon Wigner distribution in the same model using the light-front Hamiltonian perturbation theory. The state can be expanded in Fock space in terms of multiparton light-front wave functions (LFWFs) as [19]

$$|p^+,p_\perp,\sigma\rangle=\Phi^\sigma(p)b^\dagger_\sigma(p)|0\rangle+\sum_{\sigma_1\sigma_2}\int[dp_1]\int[dp_2]\sqrt{16\pi^3p^+}\delta^3(p-p_1-p_2)\Phi^\sigma_{\sigma_1\sigma_2}(p;p_1,p_2)b^\dagger_{\sigma_1}(p_1)a^\dagger_{\sigma_2}(p_2)|0\rangle, \quad (2)$$

where $[dp]=\frac{dp^+d^2p_\perp}{\sqrt{16\pi^3p^+}}$, and σ_1 and σ_2 are the helicities of the quark and gluon, respectively. The LFWFs ($\Phi^\sigma(p)$ and $\Phi^\sigma_{\sigma_1\sigma_2}$) appearing in Eq. (2) are calculated by solving the light-front eigenvalue equation in the Hamiltonian approach. $\Phi^\sigma(p)$ is the single particle (quark) LFWF and gives the wave function renormalization for the quark, and $\Phi^\sigma_{\sigma_1\sigma_2}$ is the two-particle (quark-gluon) LFWF. $\Phi^\sigma_{\sigma_1\sigma_2}(p;p_1,p_2)$ gives the probability amplitude to find a bare quark having momentum p_1 and helicity σ_1 and a bare gluon with momentum p_2 and helicity σ_2 in the dressed quark. The two-particle LFWF is related to the boost invariant LFWF: $\Psi^\sigma_{\sigma_1\sigma_2}(x,q_\perp)=\Phi^\sigma_{\sigma_1\sigma_2}\sqrt{p^+}$. Here we have used the Jacobi momenta $(x_i,q_{i\perp})$,

$$p^+_i=x_ip^+, \qquad q_{i\perp}=k_{i\perp}+x_ip_\perp, \quad (3)$$

so that $\sum_i x_i=1, \sum_i q_{i\perp}=0$. These two-particle LFWFs can be calculated perturbatively as [19]:

$$\Psi^{\sigma a}_{\sigma_1\sigma_2}(x,q_\perp)=\frac{1}{[m^2-\frac{m^2+(q_\perp)^2}{x}-\frac{(q_\perp)^2}{1-x}]}\frac{g}{\sqrt{2(2\pi)^3}}T^a\chi^\dagger_{\sigma_1}\frac{1}{\sqrt{1-x}}\left[-2\frac{q_\perp}{1-x}-\frac{(\sigma_\perp.q_\perp)\sigma_\perp}{x}+\frac{im\sigma_\perp(1-x)}{x}\right]\chi_\sigma(\epsilon_{\perp\sigma_2})^*. \quad (4)$$

We use the two-component formalism [20]. χ is the two-component fermion spinor. T^a are the usual color $SU(3)$ matrices, m is the mass of the quark, and $\epsilon_{\perp\sigma_2}$ is the polarization vector of the gluon.

The gluon-gluon correlator in Eq. (1) for a quark state dressed with a gluon can be expressed in terms of the overlap of two-particle LFWFs. The single particle sector of the Fock space expansion contributes only at $x=1$, and we exclude this.

For $\Gamma^{ij}=\delta^{ij}$, we get

$$W_1^{\sigma\sigma'}(x,k_\perp,b_\perp)=-\sum_{\sigma_1,\sigma_2,\lambda_1}\int\frac{d^2\Delta_\perp}{2(2\pi)^2}e^{-i\Delta_\perp.b_\perp}[\Psi^{*\sigma'}_{\sigma_1\lambda_1}(\hat{x},\hat{q}'_\perp)\Psi^{\sigma}_{\sigma_1\sigma_2}(\hat{x},\hat{q}_\perp)(\epsilon^1_{\sigma_2}\epsilon^{*1}_{\lambda_1}+\epsilon^2_{\sigma_2}\epsilon^{*2}_{\lambda_1})], \quad (5)$$

and for $\Gamma^{ij}=-i\epsilon^{ij}_\perp$ we get

$$W_2^{\sigma\sigma'}(x,k_\perp,b_\perp)=-i\sum_{\sigma_1,\sigma_2,\lambda_1}\int\frac{d^2\Delta_\perp}{2(2\pi)^2}e^{-i\Delta_\perp.b_\perp}[\Psi^{*\sigma'}_{\sigma_1\lambda_1}(\hat{x},\hat{q}'_\perp)\Psi^{\sigma}_{\sigma_1\sigma_2}(\hat{x},\hat{q}_\perp)(\epsilon^1_{\sigma_2}\epsilon^{*2}_{\lambda_1}-\epsilon^2_{\sigma_2}\epsilon^{*1}_{\lambda_1})], \quad (6)$$

where $\hat{x}=(1-x)$ and $\hat{q}_\perp=-q_\perp$. The Jacobi relation for the transverse momenta in the symmetric frame is given by $q'_\perp=k_\perp-\frac{\Delta_\perp}{2}(1-x)$ and $q_\perp=k_\perp+\frac{\Delta_\perp}{2}(1-x)$. We represent the gluon Wigner distribution as $W^{\lambda\lambda'}$, where λ and λ' are polarizations of the target state and gluon, respectively.

We consider only the longitudinally polarized target state and then we have four gluon Wigner distributions as follows, in a manner similar to the quark Wigner distributions [10]: the Wigner distribution of the unpolarized gluon in the unpolarized target state as

$$W^{UU}=W_1^{\uparrow\uparrow}(x,k_\perp,b_\perp)+W_1^{\downarrow\downarrow}(x,k_\perp,b_\perp), \quad (7)$$

the Wigner distribution corresponding to the distortion due to the longitudinal polarization of the target as

$$W^{LU}=W_1^{\uparrow\uparrow}(x,k_\perp,b_\perp)-W_1^{\downarrow\downarrow}(x,k_\perp,b_\perp), \quad (8)$$

the Wigner distribution corresponding to the distortion due to the longitudinal polarization of the gluons as

$$W^{UL}=W_2^{\uparrow\uparrow}(x,k_\perp,b_\perp)+W_2^{\downarrow\downarrow}(x,k_\perp,b_\perp), \quad (9)$$

and the Wigner distribution corresponding to the correlation due to the longitudinal polarization of the target state and the gluons,

$$W^{LL}=W_2^{\uparrow\uparrow}(x,k_\perp,b_\perp)-W_2^{\downarrow\downarrow}(x,k_\perp,b_\perp). \quad (10)$$

The final expressions for these four gluon Wigner distributions are given, using the two-particle LFWFs, by

$$W^{UU}(x,k_\perp,b_\perp)=N\int d\Delta_x\int d\Delta_y\frac{\cos(\Delta_\perp\cdot b_\perp)}{D(q_\perp)D(q'_\perp)}\left[\frac{-4((q_\perp q'_\perp)(x^2-2x+2)+m^2x^4)}{x^3(x-1)^2}\right], \quad (11)$$

$$W^{LU}(x,k_\perp,b_\perp)=N\int d\Delta_x\int d\Delta_y\frac{\sin(\Delta_\perp\cdot b_\perp)}{D(q_\perp)D(q'_\perp)}\left[\frac{4(2-x)(q_2q'_1-q_1q'_2)}{x^2(x-1)^2}\right], \quad (12)$$

$$W^{UL}(x,k_\perp,b_\perp)=N\int d\Delta_x\int d\Delta_y\frac{\sin(\Delta_\perp\cdot b_\perp)}{D(q_\perp)D(q'_\perp)}\left[\frac{4(x^2-2x+2)(q_2q'_1-q_1q'_2)}{x^3(x-1)^2}\right], \quad (13)$$

$$W^{LL}(x,k_\perp,b_\perp)=N\int d\Delta_x\int d\Delta_y\frac{\cos(\Delta_\perp\cdot b_\perp)}{D(q_\perp)D(q'_\perp)}\left[\frac{4((q_\perp q'_\perp)(2-x)+m^2x^3)}{x^2(x-1)^2}\right], \quad (14)$$

where A_x, A_y are x, y components of $A_\perp$ and

$$D(k_\perp)=\left(m^2-\frac{m^2+(k_\perp)^2}{1-x}-\frac{(k_\perp)^2}{x}\right), \qquad N=\frac{g^2}{2(2\pi)^2}.$$

III. GLUON GTMDS AND ORBITAL ANGULAR MOMENTUM

In order to calculate the gluon GTMDs, we use the parametrization as shown in [21], where the authors have shown that the correlators like in Eq. (1) can, in general, be written as

$$W^{O}_{\Lambda',\Lambda} = \int \frac{dz^- d^2 z_\perp}{2(2\pi)^3} e^{i\frac{xP^+}{2}z^- - i\vec{k}_\perp.\vec{z}_\perp} \langle p',\Lambda'|O(z)|p,\Lambda\rangle = \bar{u}(p',\Lambda')M^O u(p,\Lambda), \tag{15}$$

where $O(z)$ stands for the relevant quark or gluon operators and M^O stands for the matrix in Dirac space with O determined by the corresponding quark or gluon operator. The amplitude shown in Eq. (15) takes the following generic structure when the momentum transfer is purely in the transverse direction:

$$W^{\Delta S_z, c_P}_{\Lambda',\Lambda} = \frac{\bar{u}(p',\Lambda')M^{\Delta S_z, c_P}u(p,\Lambda)}{2P^+}, \tag{16}$$

where c_P is the parity coefficient of the partonic operator and ΔS_z is the spin flip number given by $\Delta S_z = \lambda' - \lambda + \Delta L_z$ such that $\lambda(\lambda')$ is the initial (final) parton light-front helicity and ΔL_z is the eigenvalue of the operator $\Delta\hat{L}_z = \hat{L}_z - \hat{L}'_z$. Also, for twist-two partonic operators, we get $\Delta L_z = 0$ and, hence, $\Delta S_z = \lambda' - \lambda$.

The gluon operators appearing in Eq. (1) correspond to the case when $\Delta S_z = 0$ and $c_P = \pm 1$ as shown in Eq. (3.12), Eq. (3.42), and Eq. (3.43) of [21]. So the relevant parametrization of the gluon GTMDs which correspond to $\Gamma^{ij} = \delta^{ij}$ in Eq. (1) is

$$M^{0,+} = \left(\frac{M}{P^+}\right)^{t-1}\left[\gamma^+\left(S^{0,+}_{t,ia} + \gamma_5 \frac{i\epsilon_T^{k_T\Delta_T}}{M^2} S^{0,+}_{t,ib}\right) + i\sigma^{j+}\left(\frac{k_T^j}{M}P^{0,+}_{t,ia} + \frac{\Delta_T^j}{M}P^{0,+}_{t,ib}\right)\right], \tag{17}$$

where

$$\epsilon_T^{ab} = \epsilon_T^{ij}a^i b^j,$$
$$\epsilon_T^{ij} = \epsilon^{-+12} = +1.$$

$t+1$ is defined as the twist of the operator in [21], so for twist two we take $t = 1$. Comparing and solving Eq. (1) and Eq. (16), we get the following expression for the gluon GTMDs:

$$S^{0,+}_{1,ia} = \frac{-2N}{D(q_\perp)D(q'_\perp)}\left[\frac{m^2x^4 + k_\perp^2(x^2-2x+2)}{x^3(x-1)^2} - \frac{\Delta_\perp^2(x^2-2x+2)}{4x^3}\right],$$

$$S^{0,+}_{1,ib} = \frac{2N}{D(q_\perp)D(q'_\perp)}\left[\frac{m^2(2-x)}{(1-x)x^2}\right],$$

$$P^{0,+}_{1,ia} = \frac{2N}{D(q_\perp)D(q'_\perp)}\left[\frac{m^2\Delta_\perp^2}{x(k_2\Delta_1 - k_1\Delta_2)}\right],$$

$$P^{0,+}_{1,ib} = \frac{2N}{D(q_\perp)D(q'_\perp)}\left[\frac{-m^2(k_\perp.\Delta_\perp)}{x(k_2\Delta_1 - k_1\Delta_2)}\right]. \tag{18}$$

The relations of these GTMDs with those in [8] are

$$S^{0,+}_{1,ia} = F^g_{1,1},$$
$$S^{0,+}_{1,ib} = F^g_{1,4},$$
$$P^{0,+}_{1,ia} = F^g_{1,2},$$
$$P^{0,+}_{1,ib} = -\frac{F^g_{1,1}}{2} + F^g_{1,3}. \tag{19}$$

So for the gluon case we get $F^g_{1,4}$ as shown below, and this relation agrees with that in [22],

$$F^g_{1,4} = \frac{N}{D(q_\perp)D(q'_\perp)}\left[\frac{m^2(2-x)}{(1-x)x^2}\right]. \tag{20}$$

From this, we can calculate the gluon canonical OAM since the canonical OAM is related to the GTMD $F_{1,4}$ as follows, similar to quarks [10,23,24]:

$$l^g_z = -\int dx d^2k_\perp \frac{k_\perp^2}{m^2}F^g_{1,4}. \tag{21}$$

This gives

$$l_z^g = -N \int dx(1-x)(2-x)[I_1 - m^2x^2I_2], \quad (22)$$

where

$$I_1 = \int \frac{d^2k_\perp}{m^2x^2 + (k_\perp)^2} = \pi log\left[\frac{Q^2 + m^2x^2}{\mu^2 + m^2x^2}\right],$$
$$I_2 = \int \frac{d^2k_\perp}{(m^2x^2 + (k_\perp)^2)^2} = \frac{\pi}{(m^2x^2)}.$$

Here Q and μ are the upper and lower limits of the $k_\perp$ integration, respectively.

For the case when $\Delta S_z = 0$ and $c_P = -1$ which corresponds to $\Gamma^{ij} = -i\epsilon_\perp^{ij}$ in Eq. (1), the relevant gluon parametrization is given by [21]

$$M^{0,-} = \left(\frac{M}{P^+}\right)^{t-1}\left[\gamma^+\gamma_5\left(S^{0,-}_{t,ia} + \gamma_5\frac{i\epsilon_T^{k_T\Delta_T}}{M^2}S^{0,-}_{t,ib}\right) + i\sigma^{j+}\gamma_5\left(\frac{k_T^j}{M}P^{0,-}_{t,ia} + \frac{\Delta_T^j}{M}P^{0,-}_{t,ib}\right)\right]. \quad (23)$$

Again by solving Eq. (23) and Eq. (1), we get the corresponding GTMDs at twist two:

$$S^{0,-}_{1,ia} = \frac{N}{D(q_\perp)D(q'_\perp)}\left[\frac{4k_\perp^2(x-2)}{2(x-1)^2x^2} + \frac{\Delta_\perp^2}{(x-1)^2x^2} - \frac{4m^2x^2 + \Delta_\perp^2(x^2-4x+5)}{2(x-1)^2x}\right],$$

$$S^{0,-}_{1,ib} = \frac{N}{D(q_\perp)D(q'_\perp)}\left[\frac{2(x^2-2x+2)m^2}{x^3(1-x)}\right],$$

$$P^{0,-}_{1,ia} = \frac{N}{D(q_\perp)D(q'_\perp)}\left[\frac{4(k_\perp.\Delta_\perp)m^2}{x(x-1)(k_2\Delta_1 - k_1\Delta_2)}\right],$$

$$P^{0,-}_{1,ib} = \frac{N}{D(q_\perp)D(q'_\perp)}\left[\frac{4k_\perp^2m^2}{x(x-1)(k_1\Delta_2 - k_2\Delta_1)}\right]. \quad (24)$$

The relations of these GTMDs with those in [8] can be written as

$$S^{0,-}_{1,ia} = 2G^g_{1,4},$$
$$S^{0,-}_{1,ib} = -G^g_{1,1},$$
$$P^{0,-}_{1,ia} = \frac{2m^2G^g_{1,2} - \Delta_\perp^2G^g_{1,1}}{2m^2},$$
$$P^{0,-}_{1,ib} = \frac{2m^2G^g_{1,3} + k_\perp.\Delta_\perp G^g_{1,1}}{2m^2}. \quad (25)$$

The spin-orbit correlation factor for the gluons C_z^g can be defined, similarly to the quark case [25], in terms of the GTMD $G^g_{1,1}$ as follows [22]:

$$C_z^g = \int dxd^2k_\perp \frac{k_\perp^2}{m^2}G^g_{1,1}. \quad (26)$$

The GTMD $G^g_{1,1}$ calculated using Eq. (25) agrees with that in [22]:

$$G^g_{1,1} = -\frac{N}{D(q_\perp)D(q'_\perp)}\left[\frac{2(x^2-2x+2)m^2}{x^3(1-x)}\right]. \quad (27)$$

So the spin-orbit correlation factor for the gluons in the dressed quark model is given by

$$C_z^g = -N\int dx\frac{2(x^2-2x+2)(1-x)}{x}[I_1 - m^2x^2I_2]. \quad (28)$$

The kinetic OAM for the gluons can be calculated using the sum rule for the gluon GPDs [3]:

$$L_z^g = \frac{1}{2}\int dx\{x[H^g(x,0,0) + E^g(x,0,0)] - \tilde{H}^g(x,0,0)\}.$$

The gluon GPDs in the above relation can be related to the GTMDs as follows:

$$H^g(x,0,t) = \int d^2k_\perp F^g_{1,1}, \quad (29)$$

$$E^g(x,0,t) = \int d^2k_\perp\left[-F^g_{1,1} + 2\left(\frac{k_\perp.\Delta_\perp}{\Delta_\perp^2}F^g_{1,2} + F^g_{1,3}\right)\right], \quad (30)$$

$$\tilde{H}^g(x,0,t) = \int d^2k_\perp G^g_{1,4}. \tag{31}$$

Using the above relation and the gluon GTMD calculated above, we can write the kinetic gluon OAM in the dressed quark model as

$$L^g_z = \frac{N}{2}\int dx\{-f(x)I_1 + 2\pi(1-x)\}, \tag{32}$$

where

$$I_1 = \int \frac{d^2k_\perp}{m^2x^2 + (k_\perp)^2} = \pi log\left[\frac{Q^2 + m^2x^2}{\mu^2 + m^2x^2}\right],$$
$$f(x) = 2x^2 - 3x + 2.$$

Unlike for the quarks in [17], the canonical gluon OAM and spin-orbit correlations are different in this model. Note that the GTMDs $F_{1,4}$ and $G_{1,1}$ depend on the gauge link.

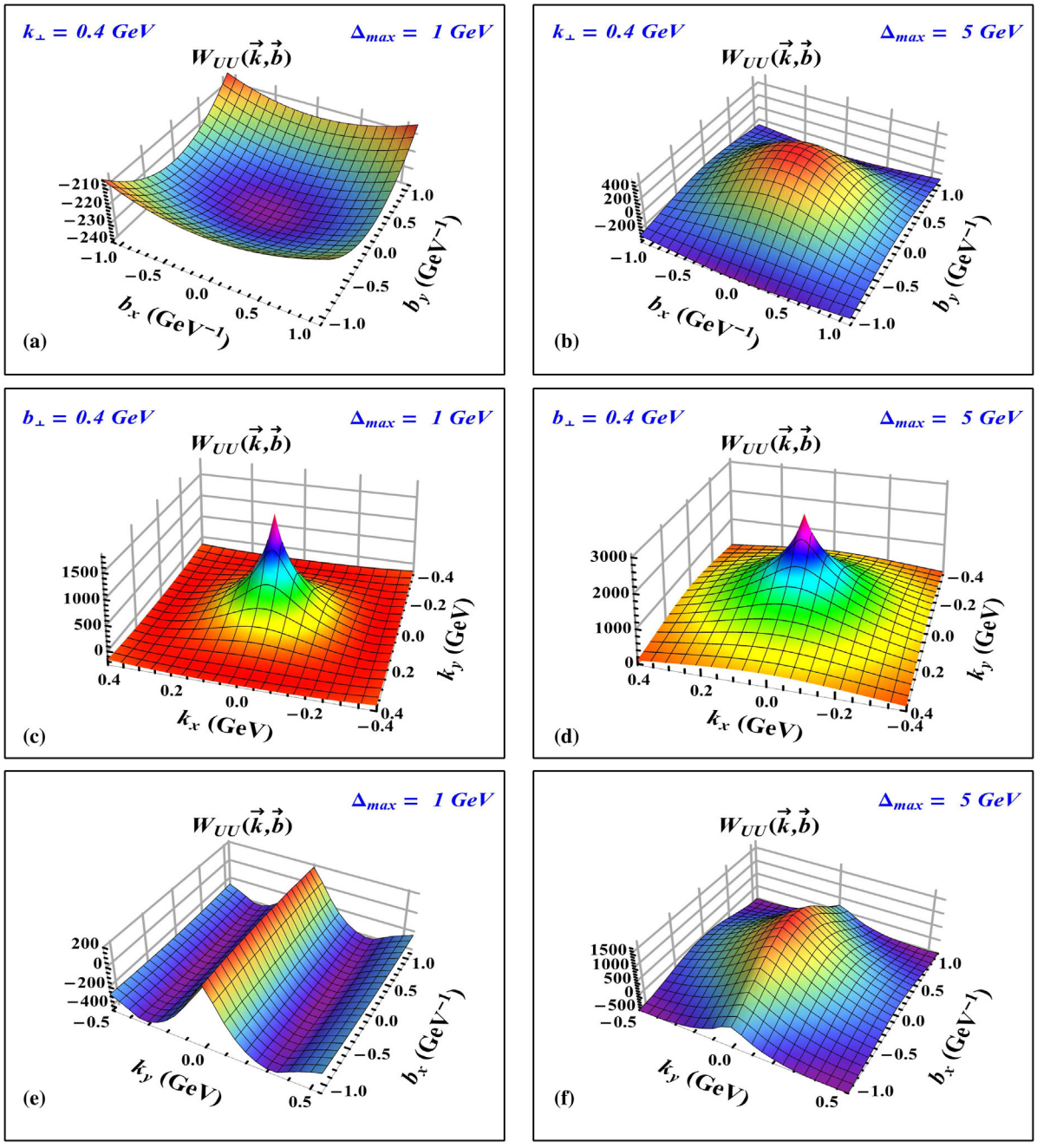

FIG. 1 (color online). Three-dimensional plots of the Wigner distributions W^{UU}. Plots (a) and (b) are in b space with $k_\perp = 0.4$ GeV. Plots (c) and (d) are in k space with $b_\perp = 0.4$ GeV^{-1}. Plots (e) and (f) are in mixed space where k_x and b_y are integrated. All the plots on the left panel (a),(c),(e) are for $\Delta_{\max} = 1.0$ GeV. Plots on the right panel (b),(d),(f) are for $\Delta_{\max} = 5.0$ GeV. For all the plots we kept $m = 0.33$ GeV, integrated out the x variable, and took $\vec{k}_\perp = k\hat{j}$ and $\vec{b}_\perp = b\hat{j}$.

But up to $O(\alpha_s)$, the result does not depend on the choice of the gauge link [22].

IV. NUMERICAL RESULTS

In Figs. 1–4, we have shown the three-dimensional plots for the Wigner distributions of the gluon in the impact parameter space $(b_x\text{-}b_y)$, momentum space $(k_x\text{-}k_y)$, and also in the mixed space $(k_y\text{-}b_x)$. Normally the upper limit of the Fourier transform should be infinite. But in our numerical calculation, we chose an upper limit of $|\Delta_\perp|$ which we called $\Delta_{\max}$. Plots on the left and right column are for $\Delta_{\max} = 1\,\text{GeV}$ and $\Delta_{\max} = 5$ GeV, respectively. The dependence of the gluon Wigner function on $\Delta_{\max}$ is similar to the quark Wigner distributions: the peak of the Wigner distribution increases in magnitude as $\Delta_{\max}$ increases. The first, second, and third rows in Figs. 1–4 correspond to the impact parameter, momentum, and mixed space plots, respectively.

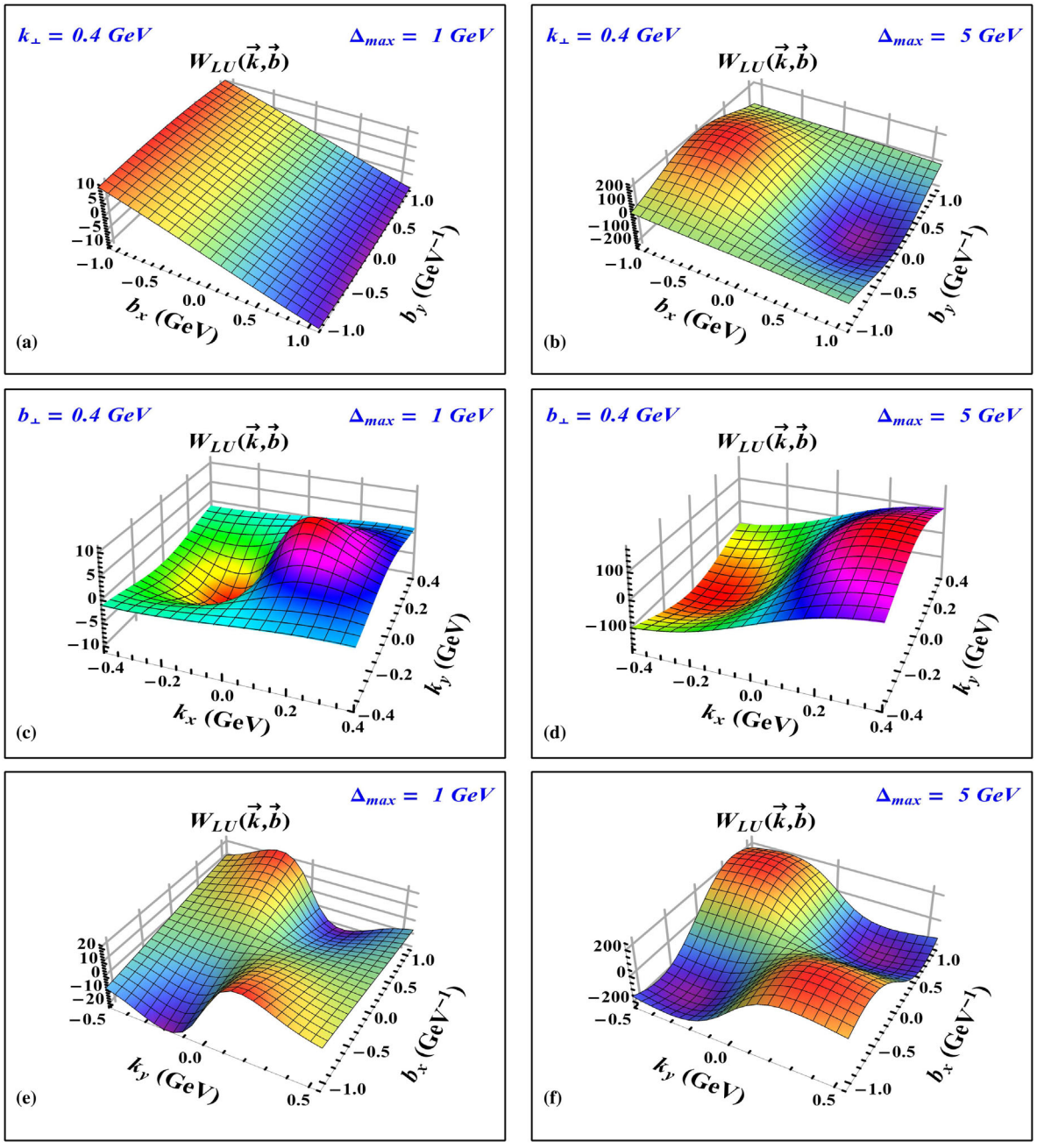

FIG. 2 (color online). Three-dimensional plots of the Wigner distributions W^{LU}. Plots (a) and (b) are in b space with $k_\perp = 0.4$ GeV. Plots (c) and (d) are in k space with $b_\perp = 0.4$ GeV^{-1}. Plots (e) and (f) are in mixed space where k_x and b_y are integrated. All the plots on the left panel (a),(c),(e) are for $\Delta_{\max} = 1.0$ GeV. Plots on the right panel (b),(d),(f) are for $\Delta_{\max} = 5.0$ GeV. For all the plots we kept $m = 0.33$ GeV, integrated out the x variable, and took $\vec{k}_\perp = k\hat{j}$ and $\vec{b}_\perp = b\hat{j}$.

The plots in mixed space have probabilistic interpretation since we have integrated out the variable in the remaining direction, i.e., k_x and b_y, and for the impact parameter and momentum space plots these remaining variables are held constant. For all the plots, we have taken the mass of the target state to be 0.33 GeV. Also, we integrated over x and divided by the normalization constant N.

In Fig. 1, we show the three-dimensional plots for the Wigner distribution of the unpolarized gluon in an unpolarized target state (W^{UU}). In Figs. 1(a) and 1(b) we see the variation of W^{UU} in the position space. The magnitude of W^{UU} is maximum at the center ($b_x = b_y = 0$) and increases with an increase in $\Delta_{\max}$, which is expected from the analytic expression of W^{UU}. In Figs. 1(c) and 1(d) we have plotted W^{UU} in the momentum space for $\vec{b}_\perp = b\hat{j} = 0.4$. In momentum space, too, W^{UU} peaks at the center ($k_x = k_y = 0$), and its magnitude increases with increasing $\Delta_{\max}$. In Figs. 1(e) and 1(f) we have shown the

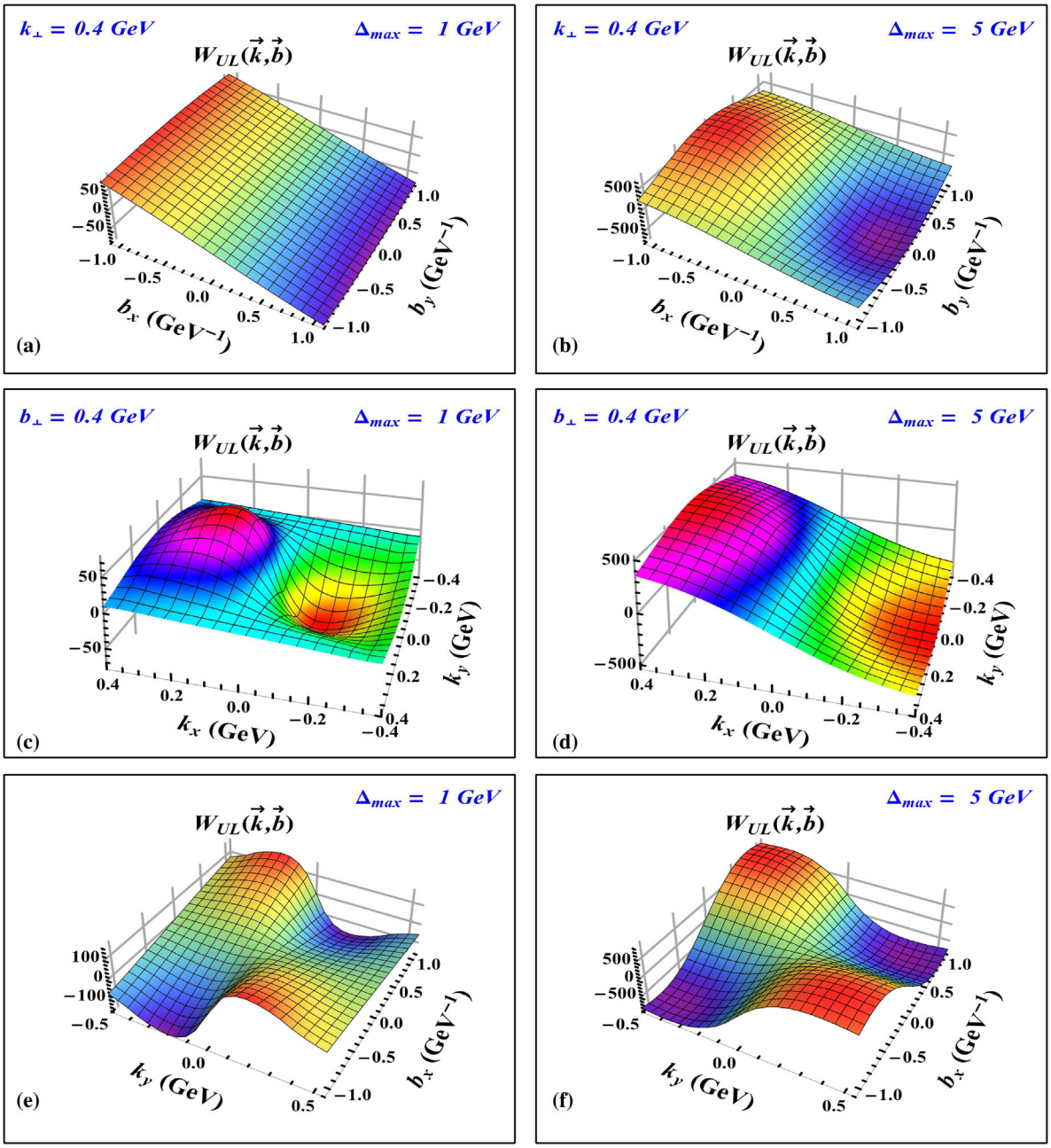

FIG. 3 (color online). Three-dimensional plots of the Wigner distributions W^{UL}. Plots (a) and (b) are in b space with $k_\perp = 0.4$ GeV. Plots (c) and (d) are in k space with $b_\perp = 0.4$ GeV^{-1}. Plots (e) and (f) are in mixed space where k_x and b_y are integrated. All the plots on the left panel (a),(c),(e) are for $\Delta_{\max} = 1.0$ GeV. Plots on the right panel (b),(d),(f) are for $\Delta_{\max} = 5.0$ GeV. For all the plots we kept $m = 0.33$ GeV, integrated out the x variable, and took $\vec{k}_\perp = k\hat{j}$ and $\vec{b}_\perp = b\hat{j}$.

variation of W^{UU} in the mixed space. We observed that W^{UU} is maximum for $k_y = 0$. As we move away from $k_y = 0$, it first decreases and then increases. Hence, the probability to find a gluon in the target state is maximum near $k_y = 0$. It is worth mentioning here that similar plots for the quark Wigner distributions in [17] are rotated through an angle $\frac{\pi}{4}$ because there we took $\Delta_\perp$ to be positive only, whereas here we took $\Delta_\perp$ to be both positive and negative.

In Fig. 2, we show the three-dimensional plots for the Wigner distribution of the unpolarized gluon in the longitudinally polarized target state. In Figs. 2(a) and 2(b) we see how W^{LU} varies in position space. We observe the dipole structure whose magnitude increases with an increase in $\Delta_{\max}$. In Figs. 2(c) and 2(d), we plotted W^{LU} in the momentum space for a fixed $\vec{b}_\perp = b\hat{j} = 0.4$. Again we observe a dipole structure, but the polarity is flipped when compared to the plots in position space. Also, the magnitude of the peak increases with increasing $\Delta_{\max}$, which is expected from the analytic expression of W^{LU}. In Figs. 2(e) and 2(f), we have shown the variation of W^{LU} in

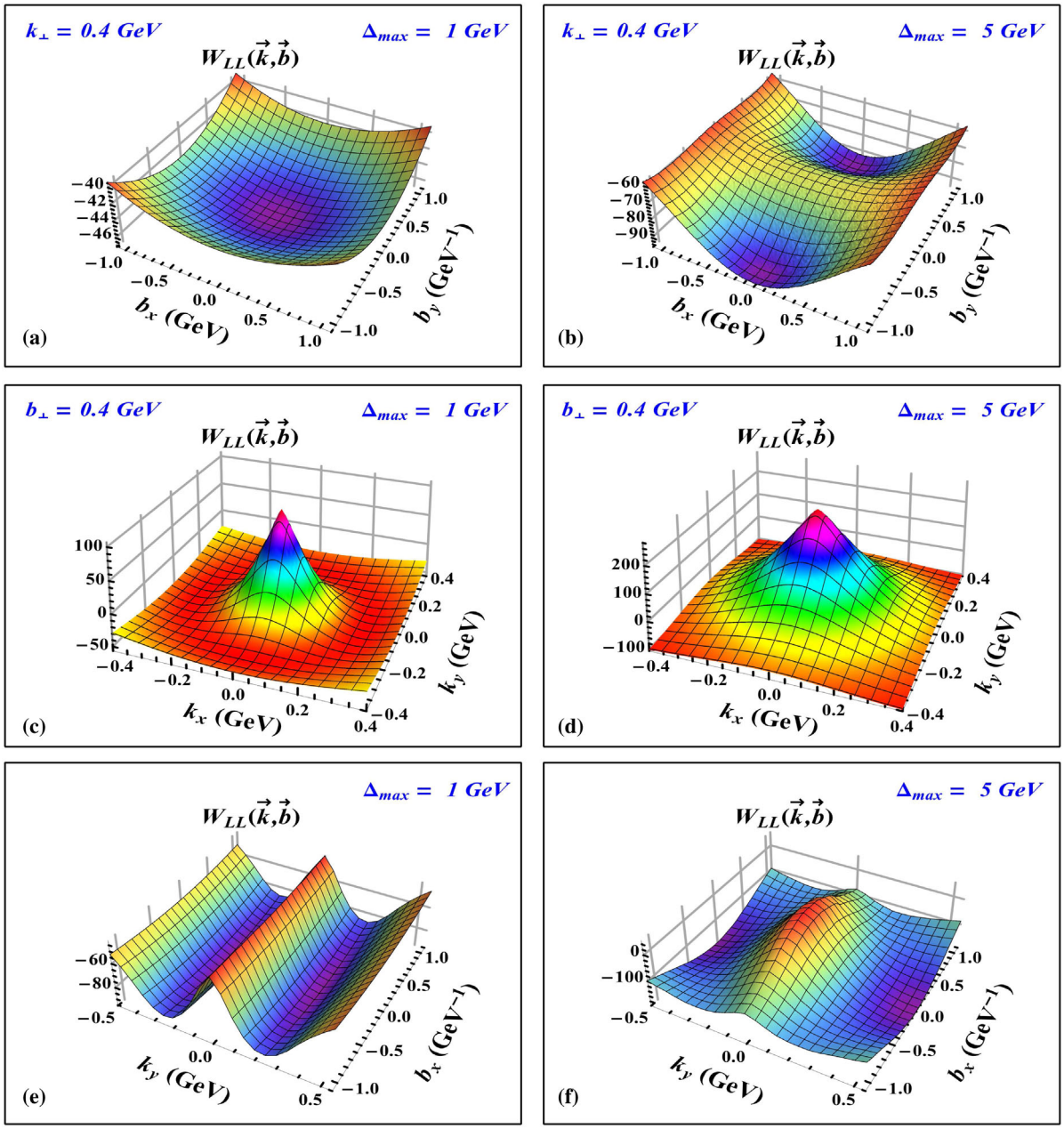

FIG. 4 (color online). Three-dimensional W^{LL}. Plots (a) and (b) are in b space with $k_\perp = 0.4$ GeV. Plots (c) and (d) are in k space with $b_\perp = 0.4$ GeV^{-1}. Plots (e) and (f) are in mixed space where k_x and b_y are integrated. All the plots on the left panel (a),(c),(e) are for $\Delta_{\max} = 1.0$ GeV. Plots on the right panel (b),(d),(f) are for $\Delta_{\max} = 5.0$ GeV. For all the plots we kept $m = 0.33$ GeV, integrated out the x variable, and took $\vec{k}_\perp = k\hat{j}$ and $\vec{b}_\perp = b\hat{j}$.

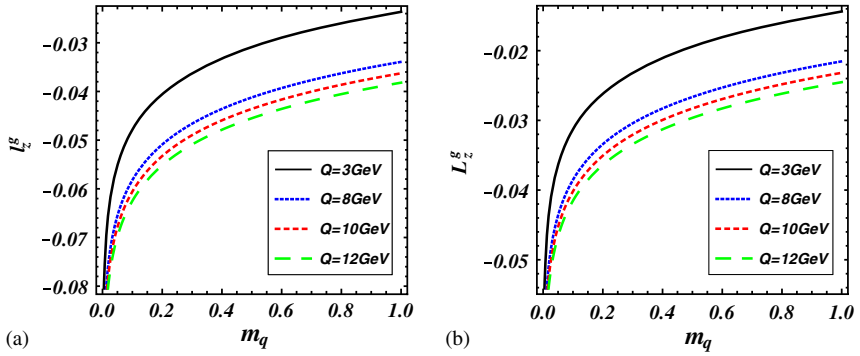

FIG. 5 (color online). Plots of OAM (a) l_z^g and (b) L_z^g vs m_q (GeV) for different values of Q (GeV).

the mixed space. Here we observe the quadrupole structure whose magnitude increases with an increase in $\Delta_{\max}$.

In Fig. 3, we show the three-dimensional plots for the Wigner distribution showing the distortion due to the longitudinal polarization of the gluons. In Figs. 3(a) and 3(b), we show that the variation of W^{UL} varies in position space for fixed $\vec{k}_\perp = k\hat{j} = 0.4$. We observe that the behavior is similar to the case of W^{LU}, showing a dipole structure. In Figs. 3(c) and 3(d), we have plotted W^{UL} in the momentum space for $\vec{b}_\perp = b\hat{j} = 0.4$. In the momentum space, we observe a dipolelike structure again similar to the case of W^{LU}, but here the polarity is not flipped, unlike that in W^{UL}, when compared to the plots in the position space. In the mixed space, we again observe a quadrupole structure with increasing magnitude as $\Delta_{\max}$ increases.

In Fig. 4, we show the three-dimensional plots for the Wigner distribution, showing the distortion due to the correlation between the longitudinal polarization of the target state and the gluons. In Figs. 4(a) and 4(b), we see how W^{LL} varies in position space. In Fig. 4(a), the $b_\perp$ space behavior is similar to that shown by W^{UU} and the magnitude increases with increasing $\Delta_{\max}$ value. In Figs. 4(c) and 4(d), we have plotted W^{LL} in the momentum space for $\vec{b}_\perp = b\hat{j} = 0.4$. In momentum space, W^{LL} shows a behavior similar to that of W^{UU}, and its magnitude increases with increasing $\Delta_{\max}$. In the mixed space again the nature is identical to that shown by W^{UU}.

In Fig. 5 we have plotted the OAM of the gluon with respect to the mass of the target state for different values of Q where Q and μ are the upper and lower limits of transverse momentum integration, respectively. μ can be taken to be zero if the quark mass is nonzero. In fact, we have taken μ to be zero. In Figs. 5(a) and 5(b), we show the canonical and the kinetic gluon OAM, respectively, as a function of the target mass. We observe that the magnitude of both the OAMs decreases with the increasing mass of the target state.

V. CONCLUSION

In this work, we presented a calculation of the gluon Wigner distributions for a quark state dressed with a gluon. This can be thought of as a simple composite spin-$\frac{1}{2}$ system having a gluonic degree of freedom. We showed the various correlations between the gluon spin and the spin of the target. We calculated the gluon kinetic and canonical OAM and also calculated the spin-orbit interaction of the gluons. The kinetic and canonical OAM of the gluons differ in magnitude. In most phenomenological models, there is no gluonic degree of freedom and a study of gluonic contribution to the spin and OAM is not possible in such models. Our simple field theoretical model calculations may be considered as a first step towards understanding the gluon spin and OAM contribution.

ACKNOWLEDGMENTS

We would like to thank C. Lorce for helpful discussions. This work is supported by the DST Project No SR/S2/HEP-029/2010, Government of India.

[1] R. L. Jaffe and A. Manohar, Nucl. Phys. **B337**, 509 (1990).
[2] X. S. Chen, W. M. Sun, X. F. Lu, F. Wang, and T. Goldman, Phys. Rev. Lett. **100**, 232002 (2008); Phys. Rev. Lett. **103**, 062001 (2009).
[3] X. Ji, Phys. Rev. Lett. **78**, 610 (1997).
[4] M. Wakamatsu, Phys. Rev. D **81**, 114010 (2010); Phys. Rev. D **83**, 014012 (2011).
[5] E. Leader and C. Lorce, Phys. Rep. **541**, 163 (2014), and the references therein.
[6] M. Burkardt, Phys. Rev. D **88**, 014014 (2013).
[7] E. P. Wigner, Phys. Rev. **40**, 749 (1932).

[8] S. Meissner, A. Metz, and M. Schlegel, J. High Energy Phys. 08 (2009) 056; S. Meissner, A. Metz, M. Schlegel, and K. Goeke, J. High Energy Phys. 08 (2008) 038.
[9] M. Burkardt, Phys. Rev. D **62**, 071503 (2000)
[10] C. Lorce and B. Pasquini, Phys. Rev. D **84**, 014015 (2011).
[11] S. Meissner, A. Metz, and K. Goeke, Phys. Rev. D **76**, 034002 (2007).
[12] A. Harindranath, in *Proc. of the International School on Light-front Quantization and Non-perturbative QCD* (International Institute of Theoretical and Applied Physics, Ames, 1997).
[13] A. Harindranath, R. Kundu, and W-M. Zhang, Phys. Rev. D **59**, 094012 (1999); **59**, 094013 (1999).
[14] S. J. Brodsky, M. Diehl, and D. S. Hwang, Nucl. Phys. **B596**, 99 (2001).
[15] S. J. Brodsky, D. Chakrabarti, A. Harindranath, A. Mukherjee, and J. P. Vary, Phys. Lett. B **641**, 440 (2006).
[16] S. J. Brodsky, D. Chakrabarti, A. Harindranath, A. Mukherjee, and J. P. Vary, Phys. Rev. D **75**, 014003 (2007).
[17] A. Mukherjee, S. Nair, and Vikash K. Ojha, Phys. Rev. D **90**, 014024 (2014).
[18] X. Ji, X. Xiong, and F. Yuan, Phys. Rev. D **88**, 014041 (2013)
[19] A. Harindranath and R. Kundu, Phys. Rev. D **59**, 116013 (1999).
[20] W-M. Zhang and Harindranath, Phys. Rev. D **48**, 4881 (1993).
[21] C. Lorce and B. Pasquini, J. High Energy Phys. 09 (2013) 138.
[22] K. Kanazawa, C. Lorce, A. Metz, B. Pasquini, and M. Schlegel, Phys. Rev. D **90**, 014028 (2014).
[23] C. Lorce, Phys. Lett. B **719**, 185 (2013)
[24] Y. Hatta, Phys. Lett. B **708**, 186 (2012).
[25] C. Lorce, Phys. Lett. B **735**, 344 (2014).